LITERATURE CITED

1. Buzyna, George, R. A. Macriss, and R. T. Ellington, *Chem. Eng. Progr. Symposium Series No. 44*, **59**, 101 (1963).
2. DeVaney, W. E., B. J. Dalton, and J. C. Meeks, *J. Chem. Eng. Data*, **8**, 473 (1963).
3. Fedoritenko, A., and M. Ruehmann, *Tech. Phys. (USSR)*, **4**, 36 (1937).
4. Gonikberg, M. G., and W. Fastovskii, *Acta Physicochim. (USSR)*, **12**, 67 (1940).
5. ———, *Foreign Pet. Technol.*, **9**, No. 6, 214 (1941).
6. Kharakhorin, F. F., *J. Tech. Phys. (USSR)*, **10**, 1533 (1940).
7. ———, *Inz.-Fiz. Z.*, **2**, No. 5, 55 (1959).
8. *Ibid.*, No. 9, 24 (1959).
9. Krichevsky, I. R., and J. S. Kasarnovsky, *J Am. Chem. Soc.*, **57**, 2168 (1935).
10. Rodewald, N. C., J. A. Davis, and Fred Kurata, *A.I.Ch.E. J.*, **10**, 937 (1964).
11. Sinor, J. E., Ph.D. thesis, Univ. Kansas, Lawrence (1965).
12. *U. S. Natl. Bureau Standards Tech. Note 154*, Dept. Commerce (1962).
13. "Open File of Information and Data Relating to the Extraction of Helium from Natural Gas by Low Temperature Processes," U. S. Bureau Mines, Amarillo, Tex. (1959).

Manuscript received August 2, 1965; revision received November 11, 1965; paper accepted November 15, 1965.

Viscosity Profiles, Discharge Rates, Pressures, and Torques for a Rheologically Complex Fluid in a Helical Flow

J. G. SAVINS and G. C. WALLICK

Socony Mobil Oil Company, Inc., Dallas, Texas

Quantitative predictions are presented to show how the axial discharge rate and pressure gradient and angular velocity and torque become coupled when a fluid exhibiting a shear-dependent viscosity behavior is subjected to a helical flow field. The numerical scheme developed here is completely general and applicable to a wide choice of constitutive equations. For purposes of illustration only, results are described for an Oldroyd type of constitutive equation. The coupling effect is illustrated for different relative speeds of the cylinders, axial flow rates, axial pressure gradients, and ratios of cylinder diameters. The most interesting consequence of the coupling effect is that the axial flow resistance is lowered in a helical flow with the result, for example, that for a given applied axial pressure gradient, the axial discharge rate in a helical flow field is higher than in a purely annular flow field.

Helical flow is a steady flow which can occur when an annular mass of fluid is contained between two coaxial cylinder of radii R_i and R ($R > R_i$) which rotate about their common axis with angular velocity Ω_1 and Ω, respectively, and a constant pressure gradient J, parallel to the axis of the cylinders, is impressed on the fluid. In a helical flow each particle describes a path about the axis of the cylinders with an angular velocity ω about the axis and a velocity u parallel to it, ω and u being functions of r only, the radial distance of the particle from the axis of the cylinders.

This multidimensional flow field is of particular interest to the experimental rheologist, since it includes as special cases each of the other viscometric flow problems for which exact solutions are known for incompressible fluids: Poiseuille flow, flow between concentric pipes, that is, annular flow, of which channel flow is a special case, and Couette flow. In principle if measurements from a given viscometric flow experiment are combined with the expressions for the stresses and the velocities to determine the material functions for, say, the *simple fluid* (*1*) or the material constants for the Oldroyd types of equations (*2*), then complete stress and velocity profiles can be predicted for helical flow or any of the other viscometric flows. A variety of treatments of the helical flow problem for rheologically complex fluids is to be found in the literature. Rivlin (*3*) introduced the term *helical* flow in a discussion of this superposition of annular and Couette flows for fluids of the differential type. However, he did not solve the resulting equations for the discharge rate and torque in terms of the applied pressure gradient, relative rotational speed, and rheological parameters. Coleman and Noll (*4*) derived such expressions. Fredrickson (*5*) used the constitutive equation devised by Rivlin, introducing a function which turns out to be simply the shear dependent viscosity function η. Coleman and Noll used the

simple fluid concept. It should be noted, however, that although the problem was attacked from different viewpoints, each approach clearly established that it is necessary to know only one material function to calculate the dependence of the velocity field in helical flow on the geometry and the applied forces. In his discussion Fredrickson outlined a feasible, although impractical method, to effect a trial-and-error solution of the nonlinear equations involved, using the shear dependent viscosity function. A theoretical and experimental treatment of helical flow based on a specialized form of the Oldroyd equation of state for incompressible elasticoviscous fluids is contained in a series of papers by Tanner (6, 7). He evaluated the relevance of Oldroyd's theoretical equation of state to the flow of real polymer solutions and obtained a solution, but only for the special limiting case of channel or plane Poiseuille flow superimposed on a Couette flow.

It is to be noted that as a result of the presence of a shear-dependent viscosity function η there is a profound difference between the helical flow of the Newtonian fluid and that of the rheologically complex fluid. The shear-dependent viscosity leads to a coupling between the superposed annular and Couette flows, and in this paper we will be concerned with quantitative predictions of how the discharge rate, pressure gradients, and the torque are affected by a helical flow produced by combining a relative rotation of the cylinders $\Delta\Omega = \Omega - \Omega_1$ and an axial pressure gradient J.

THE MATERIAL FUNCTION η

The procedure to be described here for predicting how the discharge rate and the torque are affected by a helical flow is applicable to any fluid* so long as the shear-dependent viscosity function η can be established as a known analytic function of the rate of shear Γ from an investigation of any of the viscometric flows. For purposes of illustration only, we use the particular viscometric function, Equation (2*a*). This function corresponds to various special theories of fluids, including one of those proposed by Oldroyd (2). The material function η for this equation is as follows:

$$\tau = \eta\Gamma \tag{1}$$

where

$$\eta = \eta_0 \left[\frac{1 + \sigma_2 \Gamma^2}{1 + \sigma_1 \Gamma^2} \right] \tag{2a}$$

is the expression for the shear dependent viscosity

$$\eta_0 = \int_0^\infty N(t)\,dt \tag{2b}$$

is the limiting viscosity at zero rate of shear

$$\eta_\infty = \eta_0 \frac{\sigma_2}{\sigma_1} \tag{2c}$$

is the limiting viscosity at infinite rate of shear, and

$$\sigma_1 = \frac{3}{2} \nu_1 \mu_0 \tag{2d}$$

$$\sigma_2 = \frac{3}{2} \nu_2 \mu_0 + \frac{\mu_0}{\eta_0} \left[\frac{1}{2} \theta_f \right] \eta \tag{2e}$$

The constants μ_0, ν_1, ν_2 have dimensions of time, as does $\theta_f = (\tau_{11} - \tau_{22}/\tau_{12}\,\Gamma)$ which is the natural time of the fluid (8), and $N(t)$ is the distribution function of relaxation times t. By assigning the values of $\sigma_1 = 0.06$, $\sigma_2 = 0.02$, and $\eta_0 = 10.0$ to the constants† given by Equation (2), a particular variation of the shear-dependent viscosity function characteristic of the shear thinning category of rheologically complex behavior was obtained. That is, there is a decrease in apparent viscosity from an upper limiting value at small rates of shear to a lower limiting values at high rates of shear.‡, § This constitutive equation satisfies, as pointed out later, the requirement in the helical flow solution method that the shear dependent viscosity be bounded by finite values at both low and high rates of shear.

METHOD OF SOLUTION

Mathematical Description

Both Coleman and Noll (4) and Fredrickson (5) conclude that the helical flow of any fluid|| may be characterized by two parameters which are dependent upon the pressure gradient, the angular velocity, and the shear stress-shear rate behavior of the fluid. From following the development of Fredrickson, these parameters λ^2 and C must satisfy the integral relationships

$$F_1 = \int_\alpha^1 \left(\frac{\rho^2 - \lambda^2}{\rho} \right) \frac{d\rho}{\eta} = 0 \tag{3}$$

and

$$F_2 = C \int_\alpha^1 \frac{d\rho}{\rho^3 \eta} - \Delta\Omega = 0 \tag{4}$$

The shear-dependent viscosity function η is related to the shear rate function $Y(\Gamma)$ by the equation¶

$$\eta^2 Y = 2 \left[\left(\frac{RJ}{2} \right)^2 \left(\frac{\rho^2 - \lambda^2}{\rho} \right)^2 + \frac{C^2}{\rho^4} \right] \tag{5}$$

or

$$\eta = \frac{\sqrt{\tau^2}}{\sqrt{\frac{1}{2} Y}} \tag{6}$$

where

$$\tau^2 = \tau_{r\theta}^2 + \tau_{rz}^2 \tag{7a}**$$

$$\tau_{r\theta} = \frac{C}{\rho^2} \tag{7b}$$

$$\tau_{rz} = \frac{RJ}{2} \left(\frac{\rho^2 - \lambda^2}{\rho} \right) \tag{7c}$$

$$Y(\Gamma) = 2 \left[\left(\frac{du}{dr} \right)^2 + \left(\frac{r d\omega}{dr} \right)^2 \right] \tag{7d}$$

Here τ^2 is the shear stress function and the radial position $r = \lambda R$ has the physical significance that it represents that position at which $\tau_{rz} \equiv 0$. It is evident from Equation (6) that $Y(f)$ may be considered to be equivalent to

* Actually the treatment is more restricted in that, as developed in references 4 and 5, it cannot be applied to materials which are characterized by a yield stress, for example, the Bingham types of materials.

† Unless otherwise indicated, all quantities are expressed in cgs units.

‡ In a graph of the rate of shear against shear stress, the flow curve starts as a straight line at the origin, becomes convex and then concave to the shear stress axis, and finally at the upper end becomes straight again.

§ A limitation of Equation (2*a*) is the restriction of a ratio η_∞/η_0 of 1/9. Over a sufficiently wide range it is not uncommon for a real fluid to be characterized by a ratio of 1/20 or more.

|| See the footnote in the first column.

¶ We use Y and $Y(\Gamma)$ interchangeably for the shear rate function.

** The subscript notation for cylindrical polar coordinates z, r, θ has been substituted for the 1, 2, 3 directions, respectively.

$2\Gamma^2$. If λ^2 and C have been determined, one can evaluate the angular velocity ω from

$$\omega(\rho) = \Omega - C \int_\rho^1 \frac{d\zeta}{\zeta^3 \eta} \tag{8}$$

the velocity component u in the z direction from

$$\frac{u}{R} = \frac{RJ}{2} \int_\rho^1 \left(\frac{\zeta^2 - \lambda^2}{\zeta} \right) \frac{d\zeta}{\eta} \tag{9}$$

and the actual fluid velocity V from

$$\frac{V}{R} = \left[\left(\frac{\omega}{R} \right)^2 + \rho^2 \omega^2 \right]^{1/2} \tag{10}$$

The flow rate Q is related to the parameters C, λ, and $RJ/2$ by the equation

$$F_3 = \frac{4Q}{\pi R^3} + 4 \left(\frac{RJ}{2} \right) \int_\alpha^1 \left(\frac{\alpha^2 - \rho^2}{\eta} \right) \left(\frac{\rho^2 - \lambda^2}{\rho} \right) d\rho = 0 \tag{11}$$

Here Q is defined as positive for $RJ/2 > 0$. A helical flow compounded of a plane Couette flow in one direction and a channel or plane Poiseuille flow in another direction, that is, $\alpha \cong 1$, is a special case; for example, the analysis of Tanner (*6, 7*) of this general solution which is applicable to any value of $0 < \alpha < 1$.

For a Newtonian fluid η = constant and λ^2 and C may be evaluated directly from Equations (3) and (4):

$$\lambda^2 = (\alpha^2 - 1)/(2 \ln \alpha) \tag{12}$$

and

$$C = 2\eta \, \Delta\Omega \, \alpha^2/(1 - \alpha^2) \tag{13}$$

For non-Newtonian fluids an exact solution is not possible, and it is necessary to resort to approximate numerical methods.

If the parameter $4Q/\pi R^3$ and the relative angular velocity $\Delta\Omega$ are specified, the mathematical description of the helical flow in terms of viscosity, stress, and velocity profiles requires the simultaneous solution of the three integral equations $F_i = 0$, $i = 1, 2, 3$ for the three parameters C, λ, and $RJ/2$. Flow descriptions for helical flow with $\Delta\Omega$ and $RJ/2$ specified (*4, 5*), Couette flow, and annular flow will be shown to be simplified cases of this more general treatment.

Numerical Analysis

The two characteristic parameters λ^2 and C and the pressure gradient $RJ/2$ may be evaluated numerically if the shear-dependent viscosity can be expressed as a known analytic function, for example, Equation (*2a*) or tabulated as a function of the rate of shear function $Y(\Gamma)$. Consider a table of η values corresponding to a set of tabulated $Y(\Gamma)$ values. Now η must be finite for $Y = 0$ and approach a zero or positive limit as $Y \to \infty$.* We can then generate a third table of $\eta^2 Y$ values corresponding to the Y and η tables. The η, Y data must be such that a unique value of Y corresponds to each value of $\eta^2 Y$ in the table thus formed. Now for any specified values of C, λ^2, $RJ/2$, and ρ, $\eta^2 Y$ is also determined by Equation (5). Thus the corresponding values of η required for the evaluation of Equations (3), (4), and (11) can be obtained by interpolation in the η vs. $\eta^2 Y$ tables. This η determination procedure is the foundation of the solution method developed for this study.

* These requirements are, as pointed out above, satisfied by the form of Equation (*2a*).

Since the three integral equations, $F_i = 0$, $i = 1, 2, 3$ are nonlinear in λ, C, and $RJ/2$, one must, in general, use an iterative procedure for the determination of these parameters. The Newton-Raphson method leads to three linear equations in the unknowns $\delta\lambda^2$, δC, and $\delta(RJ/2)$ of the form

$$A_{i1}\delta\lambda^2 + A_{i2}\delta C + A_{i3}\delta\left(\frac{RJ}{2}\right) = -F_i, \; (i = 1, 2, 3) \tag{14}$$

Initial values for λ^2, C, and $RJ/2$ are assumed and Equation (14) is solved for the corrections $\delta\lambda^2$, δC and $\delta(RJ/2)$. We replace λ^2 by $\lambda^2 + \delta\lambda^2$, C by $C + \delta C$, and $RJ/2$ by $RJ/2 + \delta(RJ/2)$. This solution process is repeated until $|\delta\lambda^2|$, $|\delta C|$, and $|\delta(RJ/2)|$ are all less than some specified limit or limits.

The coefficients A_{ij}, $i = 1, 2, 3$, $j = 1, 2, 3$ may be expressed in the form

$$A_{11} = \frac{\partial F_1}{\partial \lambda^2} = -\int_\alpha^1 \frac{1}{\eta\rho} \left[1 + \frac{(\rho^2 - \lambda^2)}{\eta} \frac{\partial \eta}{\partial \lambda^2} \right] d\rho \tag{15}$$

$$A_{12} = \frac{\partial F_1}{\partial C} = -\int_\alpha^1 \frac{1}{\eta\rho} \frac{(\rho^2 - \lambda^2)}{\eta} \frac{\partial \eta}{\partial C} \, d\rho \tag{16}$$

$$A_{13} = \frac{\partial F_1}{\partial (RJ/2)} = -\int_\alpha^1 \frac{1}{\eta\rho} \frac{(\rho^2 - \lambda^2)}{\eta} \frac{\partial \eta}{\partial (RJ/2)} \, d\rho \tag{17}$$

$$A_{21} = \frac{\partial F_2}{\partial \lambda^2} = -C \int_\alpha^1 \frac{1}{\eta^2 \rho^3} \frac{\partial \eta}{\partial \lambda^2} \, d\rho \tag{18}$$

$$A_{22} = \frac{\partial F_2}{\partial C} = \int_\alpha^1 \frac{1}{\eta\rho^3} \left[1 - \frac{C}{\eta} \frac{\partial \eta}{\partial C} \right] d\rho \tag{19}$$

$$A_{23} = \frac{\partial F_2}{\partial (RJ/2)} = -C \int_\alpha^1 \frac{1}{\eta^2 \rho^3} \frac{\partial \eta}{\partial (RJ/2)} \, d\rho \tag{20}$$

$$A_{31} = \frac{\partial F_3}{\partial \lambda^2} = -4\left(\frac{RJ}{2}\right) \int_\alpha^1 \frac{\alpha^2 - \rho^2}{\eta\rho} \left\{ 1 + \frac{(\rho^2 - \lambda^2)}{\eta} \frac{\partial \eta}{\partial \lambda^2} \right\} d\rho \tag{21}$$

$$A_{32} = \frac{\partial F_3}{\partial C} = -4\left(\frac{RJ}{2}\right) \int_\alpha^1 \frac{(\alpha^2 - \rho^2)}{\eta\rho} \frac{(\rho^2 - \lambda^2)}{\eta} \frac{\partial \eta}{\partial C} \, d\rho \tag{22}$$

and

$$A_{33} = \frac{\partial F_3}{\partial (RJ/2)} = 4 \int_\alpha^1 \frac{(\alpha^2 - \rho^2)}{\eta\rho} (\rho^2 - \lambda^2) \, d\rho - 4\left(\frac{RJ}{2}\right) \int_\alpha^1 \frac{(\alpha^2 - \rho^2)}{\eta\rho} \frac{(\rho^2 - \lambda^2)}{\eta} \frac{\partial \eta}{\partial (RJ/2)} \, d\rho \tag{23}$$

The partial derivatives appearing in Equations (15) to (23) cannot be evaluated directly. We can, however, write

$$\frac{\partial \eta}{\partial \lambda^2} = \frac{\partial (\eta^2 Y)}{\partial \lambda^2} \frac{\partial \eta}{\partial (\eta^2 Y)} = -4\left(\frac{RJ}{2}\right)^2 \left(\frac{\rho^2 - \lambda^2}{\rho}\right) \frac{\partial \eta}{\partial (\eta^2 Y)} \tag{24}$$

$$\frac{\partial \eta}{\partial C} = \frac{\partial(\eta^2 Y)}{\partial C}\,\frac{\partial \eta}{\partial(\eta^2 Y)} = \frac{4C}{\rho^4}\,\frac{\partial \eta}{\partial(\eta^2 Y)} \tag{25}$$

and

$$\frac{\partial \eta}{\partial(RJ/2)} = \frac{\partial(\eta^2 Y)}{\partial(RJ/2)}\,\frac{\partial \eta}{\partial(\eta^2 Y)} = 4\left(\frac{RJ}{2}\right)\left(\frac{\rho^2-\lambda^2}{\rho}\right)^2 \frac{\partial \eta}{\partial(\eta^2 Y)} \tag{26}$$

The necessary $\partial\eta/\partial(\eta^2 Y)$ may be evaluated by numerical interpolation and differentiation in the η, $\eta^2 Y$ tables. For example, one could establish a table of $\partial\eta/\partial(\eta^2 Y)$ values corresponding to the tabulated values of η and $\eta^2 Y$. The value of $\partial\eta/\partial(\eta^2 Y)$ corresponding to a specific value of $\eta^2 Y(\rho, RJ/2, \lambda^2, C)$ could then be obtained by direct interpolation. The F_i and A_{ij} are evaluated by standard numerical integration procedures.

If the pressure gradient $RJ/2$ is specified rather than $4Q/\pi R^3$, that is, the special case considered by Coleman and Noll (*4*) and Fredrickson (*5*), the problem reduces to the simultaneous solution of Equations (3) and (4) for the parameters λ^2 and C. The Newton-Raphson procedure leads to two equations of the form

$$A_{i1}\delta\lambda^2 + A_{i2}\delta C = -F_i, \quad i = 1, 2 \tag{27}$$

where the A_{ij} are defined in Equations (15), (16), (18), and (19).

For annular flow $\Delta\Omega = C = 0$, the determination of $RJ/2$ and λ^2 corresponding to a specified flow rate requires the repetitive solution of the equations

$$A_{i1}\delta\lambda^2 + A_{i3}\delta\left(\frac{RJ}{2}\right) = -F_i, \quad i = 1, 3 \tag{28}$$

where the A_{ij} are defined in Equations (15), (17), (21), and (23). If $RJ/2$ is known, only λ^2 must be determined and we have simply

$$A_{11}\delta\lambda^2 = -F_1 \tag{29}$$

For Couette flow $RJ/2 = \lambda^2 = 0$, the parameter C corresponding to any imposed $\Delta\Omega$ may be evaluated by the iterative solution of Equation (4) through the derived equation

$$A_{22}\delta C = -F_2 \tag{30}$$

with A_{22} as defined in Equation (19). If we specify the torque at $\rho = \alpha$ or $\rho = 1$ rather than $\Delta\Omega$, C follows immediately from Equation (7*b*). The relative angular velocity $\Delta\Omega$ and the several viscosity, stress, and velocity profiles may then be evaluated directly without iteration.

While the general solution procedure as outlined above is normally rapidly convergent, solution oscillation may occasionally be encountered. For such cases the procedure is modified by restricting acceptable δC, $\delta\lambda^2$, and $\delta(RJ/2)$ to those tending to minimize the $|F_1|$, $|F_2|$, and $|F_3|$. If computed values of δC and $\delta\lambda^2$ are such as to increase the magnitude of F_1 and F_2, we replace δC and $\delta\lambda^2$ by $\frac{\delta C}{2}$ and $\frac{\delta\lambda^2}{2}$ and repeat the test until the minimization condition has been satisfied. From 10 to 60 sec.* are required to evaluate a set of λ^2, C, and $RJ/2$ values and to tabulate complete stress and velocity profiles.

Helical Flow Simulation

By using the method of solution outlined in the preceding discussion, the following helical flow problems were simulated:

1. An annular flow on which is superimposed varying degrees of Couette flow by relative rotations of one cylinder with respect to the other.
2. A Couette flow on which is superimposed varying degrees of annular flow by applying a series of axial pressure gradients. Cases 1 and 2 were evaluated for several ratios of inner to outer cylinder radii: $\alpha = 0.95$, 0.80, and 0.50. In case 1 a series of discharge rates and profiles of η in ρ was computed for specified values of the parameter $RJ/2$, that is corresponding to different values of the axial pressure gradient, for a given α, to first establish the conditions in annular flow for zero relative rotation, that is, zero torque. The computations were then repeated for the same range in $RJ/2$ and α for a specified relative rotation $\Delta\Omega$, and a series of helical flow discharge rates, torques, and the corresponding profiles of η in ρ were determined. The same procedure was followed for different values of $\Delta\Omega$ and α. Additionally, for a given α, a series of axial pressure gradients and profiles of η in ρ were computed for specified values of the parameter $4Q/\pi R^3$ for a specified relative rotation $\Delta\Omega$. For case 2 a series of torques and profiles of η in ρ were first computed for specified values of $\Delta\Omega$ to establish the conditions in Couette flow for zero flow, that is, zero axial pressure gradient. The calculations were then repeated for a specified value of $RJ/2$ for the same range in $\Delta\Omega$ and α, and a series of torques, discharge rates, and corresponding profiles of η in ρ in a helical flow were determined. This procedure was repeated for different values of $RJ/2$ and α.

RESULTS AND DISCUSSION

Viscosity Profiles in Nonhelical Flows

The basic characteristics of annular and Couette flows are already well known and therefore will not be considered in detail. However, the characteristics of the shear stresses are worth noting, because their distribution within the shear region $\alpha < \rho < 1$ affects the variation of the apparent viscosity function η over that region, that is, resulting in the appearance of a viscosity profile in ρ. It is this variation which accounts for the profound differences between Newtonian and rheologically complex fluids in a helical flow. Equation (7*b*) shows that in Couette flow $(\tau_{r\theta})_{\rho=\alpha}$, the shear stress at the inner wall, is related to $(\tau_{r\theta})_{\rho=1}$, the shear stress at the outer wall, in the following manner:

$$(\tau_{r\theta})_{\rho=1} = \alpha^2\,(\tau_{r\theta})_{\rho=\alpha} \tag{31}$$

Equation (31) shows that the shear stress in Couette flow is larger at the inner wall. Additionally, $\tau_{r\theta}$ is always finite, and the amount of the decrease with increasing radial distance obviously depends upon the parameter $\left(\frac{\alpha}{\rho}\right)^2$. The same conclusions apply to the variation with radial position of the parameter $Y/2$, since the latter can be regarded as a function of the shear stress.

Annular flow is significantly different from the Couette type of flow, because the shear stress τ_{rz} vanishes at the position $\rho = \lambda$. It follows from the first-order differential equation for the shear stress distribution across the annulus, Equation (7*c*), that $(\tau_{rz})_{\rho=\alpha}$ and $(\tau_{rz})_{\rho=1}$ are related in the following way:

$$(\tau_{rz})_{\rho=1} = (1-\lambda^2)\left(\frac{\alpha}{\alpha^2-\lambda^2}\right)(\tau_{rz})_{\rho=\alpha} \tag{32}$$

and since $\lambda > \alpha$ these stresses must be of opposite sign. From these results the shear stress distribution across the region $\alpha < \rho < 1$ can be summarized as follows: $|(\tau_{rz})|$ is larger at the inner wall; the magnitude of the stress decreases in the interval $\alpha < \rho < \lambda$, vanishing at the position $\rho = \lambda$; the stress then increases in magnitude in the

* With a CDC 1604 digital computer.

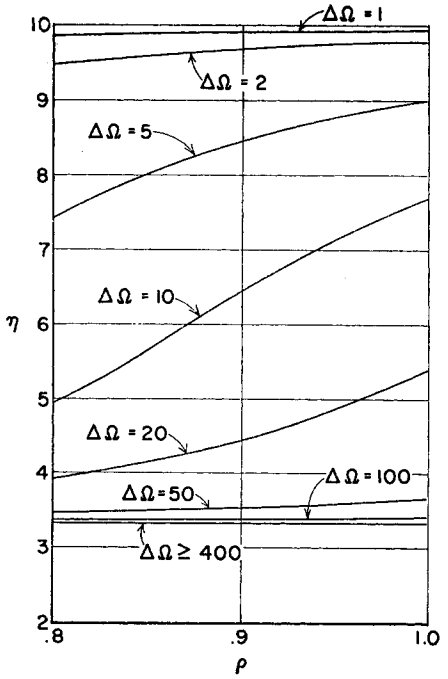

Fig. 1. Viscosity profiles in Couette flow for various relative speeds ($\alpha = 0.80$).

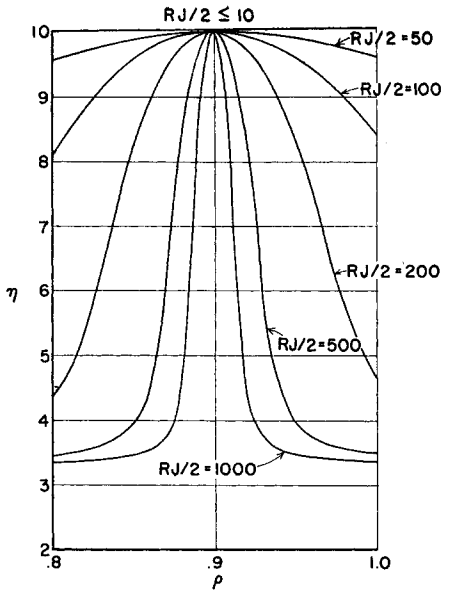

Fig. 2. Viscosity profiles in annular flow for various values of $RJ/2$ ($\alpha = 0.80$).

interval $\lambda < \rho < 1$ to a finite value at the outer wall $|(\tau_{rz})_{\rho=1}| < |(\tau_{rz})_{\rho=\alpha}|$. The same conclusions apply to the variation of the rate of shear with position for reasons outlined above. These shear stress (or rate of shear) distributions are reflected in the appearance of a profile in ρ of the shear-dependent viscosity η within the region $\alpha < \rho < 1$.

Viscosity profiles, that is, graphs of η vs. ρ have been drawn up for $\alpha = 0.80$ using the previously cited values for σ_1, σ_2, and η_0. Typical Couette flow viscosity profiles for zero axial pressure gradient are illustrated in Figure 1 for several values of the relative rotation* $\Delta\Omega$. Annular flow viscosity profiles for zero torque are illustrated in Figure 2 for several values of the parameter $RJ/2$. There is only a qualitative similarity between the profiles for the two flows in the region of low shear rates and shearing stresses, that is $\Delta\Omega \leqq 2$ and $RJ/2 \leqq 50$. Gross differences arise at larger values of these parameters. For example, in Couette flow at $\Delta\Omega \leqq 2$, η approaches η_0, the limiting viscosity at zero rate of shear, while for $\Delta\Omega \geqq 400$ the limiting viscosity at infinite rate of shear is approached. At intermediate values of $\Delta\Omega$, the shear-dependent behavior of η as expressed by Equation (2*a*) is quite pronounced. Note that irrespective of the value of $RJ/2$, the zero rate of shear viscosity always occurs in the profile for annular flow at the position $\rho = \lambda$, that is, $\eta_{\rho=\lambda} \equiv \eta_0$. It is also worth noting that the position λ is remarkably insensitive to $RJ/2$. For the example shown in Figure 2, within the range $50 < RJ/2 < 1{,}000$, the shift is on the order of 0.01%, with λ displaced first in the $-\rho$ direction for small $RJ/2$ and then in the $+\rho$ direction for large $RJ/2$. Note that for $RJ/2 \geqq 1{,}000$, η approaches the limiting viscosity at infinite rate of shear.

Effect of a Helical Flow on Viscosity Profiles

When the Couette and annular flows are combined to produce a helical flow, the shear stresses $\tau_{r\theta}$ and τ_{rz} form the shear stress function τ^2, given by Equation (7*a*), which profoundly alters the characteristics of the viscosity profile within the region $\alpha < \rho < 1$. Helical flow viscosity profiles for $\alpha = 0.80$, have been drawn up for cases 1 and 2. Viscosity profiles for case 1 for $RJ/2 = 500$ and several values of the parameter $\Delta\Omega$ are illustrated in Figure 3, while viscosity profiles corresponding to case 2 for $\Delta\Omega = 10$ and several values of the parameter $RJ/2$, that is, for a range in axial pressure gradients, are shown in Figure 4. The most striking result of combining the flows is to shift the η function toward smaller values. Thus, although the physical significance of λ is retained, it follows from Equation (7*a*) that the effective shear stress τ^2 does not vanish at $\rho = \lambda$ but instead one obtains the result $\tau^2_{\rho=\lambda} = \tau^2_{r\theta}$. Since $\tau_{r\theta}$ is finite for $\Delta\Omega \geqq 0$ it follows that the limiting viscosity at zero rate of shear, that is, η_0 can never occur in a helical flow viscosity profile. This

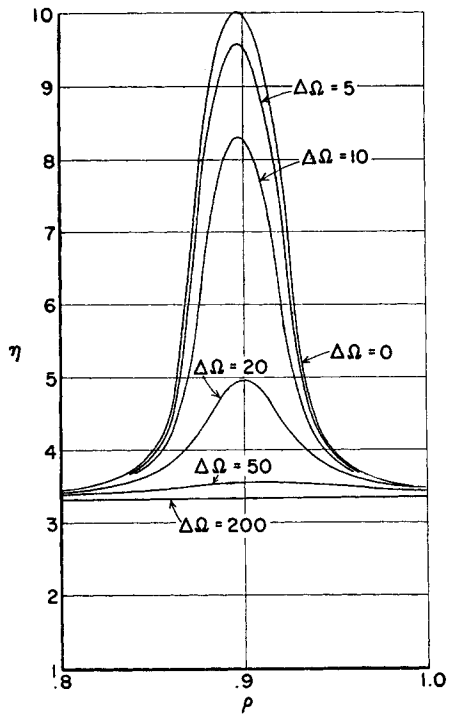

Fig. 3. Viscosity profiles in helical flow for $RJ/2 = 500$ and various relative speeds ($\alpha = 0.80$).

* In all examples to follow, the parameter $\Delta\Omega$ is expressed in rev./min.

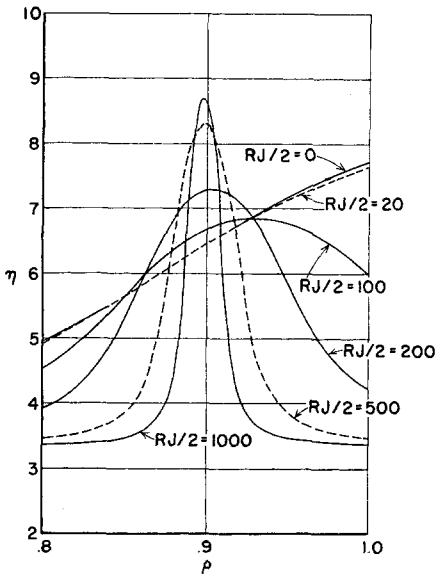

Fig. 4. Viscosity profiles in helical flow for $\Delta\Omega = 10$ and various values of $RJ/2$ ($\alpha = 0.80$).

result has an important bearing on helical flow as will be shown later.

There are some interesting differences between the case 1 and case 2 viscosity profiles which are worth noting because of their consequences on the discharge rate and torque in helical flow. Figure 3 shows that the effect of impressing a relative rotation on annular flow is to decrease the shear-dependent viscosity everywhere within the region $\alpha < \rho < 1$, with the result that the flow resistance in the axial direction is also decreased. This is a result which one might anticipate from purely intuitive notions for this category of rheologically complex fluids. However, in case 2 the effect of impressing an axial pressure gradient on a Couette flow is more complicated. The shear-dependent viscosity may be lower in certain areas and higher elsewhere. Figure 4 shows that as $RJ/2$ increases, η is considerably reduced near the cylinder walls. However, there is also a pronounced increase in η at the other radial positions. The striking maximum in η, which occurs near the position $\rho = \lambda$, is accentuated with increasing $RJ/2$.* However, the overall effect in case 2 leads to the same result obtained for case 1, which is that the axial resistance to flow is reduced in a helical flow.

Effect of a Helical Flow on Axial Discharge Rates, Pressures, and Torques

Predictions for case 1 helical flow are summarized in Figure 5 for $\Delta\Omega = 10$, 300, and $\alpha = 0.50$, 0.80, 0.95. The parameter Q/Q_0 is the ratio of the discharge rate in helical flow to the discharge rate in annular flow compared at identical values of $RJ/2$ and α. It is seen that the effect of a helical flow produced by impressing a relative rotation on the z directed annular flow is to increase the axial discharge rate. This result is not unexpected. The preceding viscosity profile analyses showed that the shear-dependent viscosity is lowered, hence the axial flow resistance is lowered, by the effective shear stress τ^2 which is characteristic of a helical flow. Note that Q/Q_0 is considerably higher for conditions of large α and high relative speeds. For instance in Figure 5 at $RJ/2 = 100$, $Q = 3Q_0$ at $\alpha = 0.95$, while at $\alpha = 0.50$, $Q = 1.41Q_0$. Additionally, it is to be noted that, although the increased discharge rate persists to higher values of $RJ/2$ for, say, $\alpha = 0.95$, a point will eventually be reached where a discharge rate characteristic of annular flow for zero torque will be obtained. Figure 6 illustrates how the axial pressure gradient required to maintain a specified axial flow rate is affected by different values of the imposed relative rotation of the cylinders. The parameter J/J_0 is the ratio of the pressure in helical flow to the pressure in annular flow compared at $\alpha = 0.80$. The specified values for $4Q/\pi R^3$, that is, 0.005, 0.10, may be regarded as relative measures of the axial flow rate. One notes that an appreciable reduction in axial pressure gradient occurs with relative rotation. The effect is somewhat suppressed at the higher flow rate. At $\Delta\Omega = 60$ rev./min., for example, comparing the pressure gradient ratios at the indicated levels of $4Q/\pi R^3$, the percent reduction in axial pressure gradient which results with relative rotation is decreased slightly from 65 to 62% although the flow rates differ by a factor of 20. The flow behavior at $\alpha = 0.95$ is similar, but the pressure gradient reduction is more pronounced for small relative rotations.†

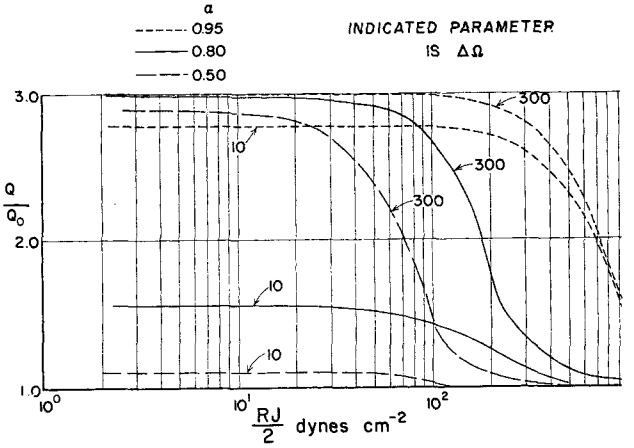

Fig. 5. Effect of helical flow on annular discharge rate for $\Delta\Omega = 10$, 300 and $\alpha = 0.50$, 0.80, 0.95.

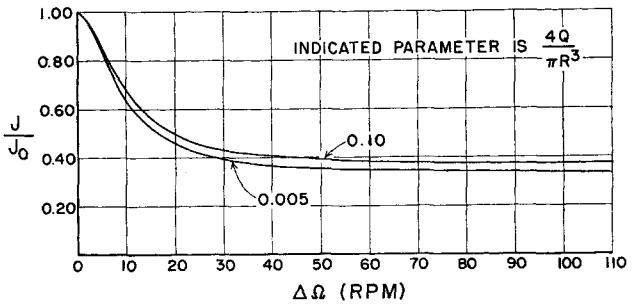

Fig. 6. Effect of helical flow on axial pressure gradient for $\alpha = 0.80$, $4Q/\pi R^3 = 0.005$, 0.10.

* The observation that the maximum value of η occurs near $\rho = \lambda$ can be stated more precisely. Differentiating Equation (5) with respect to ρ one obtains:

$$\lambda^4 = \rho_m{}^4 - \frac{8}{\rho_m{}^2}\left[\frac{C}{RJ}\right]^2$$

where ρ_m is the radial position where the maximum value of η occurs for any compatible values of λ and $8\left[\frac{C}{RJ}\right]^2$ satisfying Equations (3) and (4). This result shows that $\rho = \lambda$ will always lie to the left of ρ_m and further, as $\frac{RJ}{2}$ increases, there will be less difference between λ and ρ_m.

† It is apparent that the power required to maintain a given flow rate is changed by imparting a tangential component to the flow. It is anticipated that both the magnitude and direction of this change will depend upon the detailed properties of the fluid of interest and design conditions, for example, geometry, angular velocity, axial pumping conditions, etc.

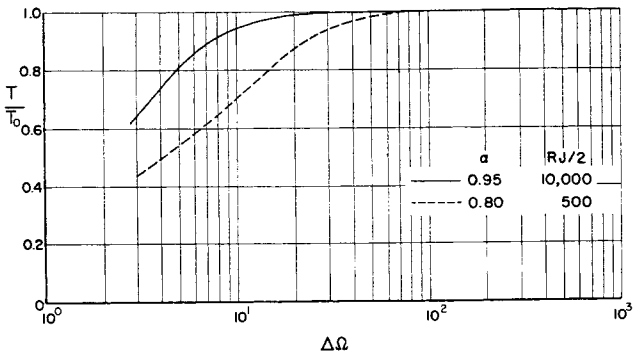

Fig. 7. Effect of helical flow on torque for $RJ/2 = 500$, 10,000 and $\alpha = 0.80$, 0.95.

Predictions for case 2 helical flow are summarized in Figure 7 for $\alpha = 0.95$, $RJ/2 = 10^4$, and $\alpha = 0.80$, $RJ/2 = 500$. The quantity T/T_0 is the ratio of the torque in a helical flow to the torque in a Couette flow compared at identical values of $\Delta\Omega$ and α. These results show that impressing a z directed annular flow on a Couette flow leads to a coupling between the shear dependent viscosity and the torque with the result that a significant lowering of the torque occurs in a helical flow. Note that the reduction in torque is more pronounced for $\alpha = 0.80$ for a considerably smaller value of $RJ/2$. As the relative speed is increased, the effect of the impressed annular flow becomes less significant and a torque characteristic of Couette flow for zero axial pressure gradient is eventually obtained.

It is to be noted that these results should not be interpreted as the typical behavior of *any* rheologically complex fluid in a helical flow. The fact that the discharge rate is increased, the torque lowered, and the viscosity profile shifted toward a smaller scale results from the *choice of viscosity function.*

SUMMARY

A numerical scheme has been developed for quantitatively predicting the dependence of the axial discharge rate and the torque on the shear-dependent viscosity function η for a rheologically complex fluid and the stress field in a helical flow, that is, a fluid motion imparted by a simultaneously occurring steady z directed annular flow and a steady relative rotation about the z axis.

For purposes of illustration only, solutions are described for an Oldroyd type of constitutive equation, for which $\eta = \eta_0 \left[\frac{1 + \sigma_2 \Gamma^2}{1 + \sigma_1 \Gamma^2} \right]$ for different relative speeds, axial flow rates, pressure gradients, and ratio of cylinder diameters. The analysis shows that in a helical flow the profile of η in the reduced radial coordinate ρ is shifted toward a smaller scale than obtained in either the zero axial pressure gradient or zero torque flows. This interaction between η, as defined above, and the helical flow stress field results in a *lowering of the axial flow resistance.* Hence the axial discharge rate is increased, and the axial pressure and torque lowered in a helical flow. In contrast, if the fluid were Newtonian the superimposed laminar flows would be noninterfering in that there would be no coupling among the discharge rate, axial pressure gradient, relative rotation, and torque through the viscosity coefficient.

The solution method is completely general and applicable to any choice of constitutive equation provided it is of the type such that η is finite for $Y(f) = 0$ and approaches a zero or positive limit at $Y(f) \to \infty$.

ACKNOWLEDGMENT

The authors wish to express their appreciation to the Socony Mobil Oil Company, Inc., for permission to publish this paper. Also, we wish to thank Professor C. Truesdell, Johns Hopkins University, and Professor A. Fredrickson, University of Minnesota, for comments in connection with the review of the manuscript.

NOTATION

$A_{ij}(i = 1,2,3,\ j = 1,2,3)$ = coefficients defined by Equations (15) to (23)
C = helical flow parameter, defined by Equation (4)
$F_j(i = 1,2,3)$ = functions defined by Equations (3), (4), (11)
J, J_0 = pressure gradients, helical and annular flows, respectively
$N(t)$ = relaxation spectrum
Q, Q_0 = axial discharge rate, helical and annular flows, respectively
r = radial coordinate
R, R_i = radius of outer and inner cylinders, respectively
T, T_0 = torques, helical and Couette flows, respectively
u = velocity component in z direction
V = actual fluid velocity
$Y, Y(f)$ = shear rate function, defined by Equation (7*d*), equal to $2\Gamma^2$

Greek Letters

α = R_i/R
Γ = shear rate
δ = incremental change in indicated parameter
ζ = dummy variable of integration
η = shear-dependent viscosity function, defined by Equation (2*a*)
η_0 = limiting viscosity at zero rate of shear, defined by Equation (2*b*)
η_∞ = limiting viscosity at infinite rate of shear, defined by Equation (2*c*)
λ = helical flow parameter defined by Equation (3)
μ_0 = constant in Equation (2*d*)
θ_f = fluid natural time
ν_1, ν_2 = constants in Equations (2*d*) and (2*e*), respectively
ρ = reduced radial coordinate, equal to r/R
σ_1, σ_2 = constants in Equation (2*c*)
$\tau, \tau_{21}, \tau_{r\theta}, \tau_{rz}$ = shear stress
$\tau_{11}, \tau_{22}, \tau_{33}$ = physical components of the stress tensor parallel to the streamlines, normal to the shearing surfaces, and normal to surfaces normal to the shearing surfaces
τ^2 = shear stress function, defined by Equation (7*a*)
$\omega, \omega(\rho)$ = angular velocity
Ω, Ω_1 = angular velocity of outer and inner cylinders, respectively
$\Delta\Omega$ = $\Omega - \Omega_1$

LITERATURE CITED

1. Coleman, B. D., and W. Noll, *Ann. N. Y. Acad. Sci.*, **89**, No. 4, 573 (1961).
2. Oldroyd, J. G., *Proc. Royal Soc. (London)*, **A245**, 278 (1958).
3. Rivlin, R. S., *J. Ratl. Mech. Anal.*, **5**, 179 (1956).
4. Coleman, B. D., and W. Noll, *J. Appl. Phys.*, **30**, 1508 (1959).
5. Fredrickson, A. G., *Chem. Eng. Sci.*, **11**, 252 (1960).
6. Tanner, R. I., *Rheol. Acta*, **3**, 23 (1963).
7. *Ibid.*, 26.
8. Truesdell, C., *Phys. Fluids*, **7**, 1134 (1964).

Manuscript received July 24, 1965; revision received November 8, 1965; paper accepted November 9, 1965. Paper presented at A.I.Ch.E. Philadelphia meeting.